Effects of pressure on charge transport and magnetic properties of La$_{1.32}$Sr$_{1.68}$Mn$_2$O$_7$ layered manganite

M. Kumaresavanji,[1,a)] M. S. Reis,[2] Y. T. Xing,[1] and M. B. Fontes[1]

[1]*Centro Brasileiro de Pesquisas Fisicas, Rua Dr. Xavier Sigaud 150, Urca, 22290-180 Rio de Janeiro, Brazil*
[2]*CICECO, University of Aveiro, 3810-193 Aveiro, Portugal*

We have studied the effects of hydrostatic pressure on the electrical transport and magnetic properties of La$_{1.32}$Sr$_{1.68}$Mn$_2$O$_7$ layered manganite up to 25 kbars. At ambient pressure, the compound exhibits a ferromagnetic transition accompanied by a metal-insulator transition (T_{MI}^1) at 118 K. Increasing pressure induces a second metal-insulator (T_{MI}^2) transition at a critical pressure of $6 \leq P_C \leq 7$ kbars in the temperature dependence of resistivity measurement. With further increase in pressure, both T_{MI}^1 and T_{MI}^2 shift to higher temperatures continuously, however, displaying a suppression in the amplitude of the peaks on the resistivity curves. We could not observe any transition corresponding to T_{MI}^2 in the temperature dependence of magnetization measurement under pressures up to 10 kbars. However, pressure reduces the magnetic moments at low temperatures and shifts the T_C to higher temperatures at the same rate observed for T_{MI}^1. A large negative tunneling magnetoresistance was observed around T_C due to the applied magnetic field up to the maximum available value of 5 T, and the pressure reduces the magnetoresistance ratio significantly. This result is due to the canted ferromagnetic order that was established by increasing pressure, which leads to an electron localized ferromagnetic insulating phase. © *2009 American Institute of Physics*. [doi:10.1063/1.3256182]

I. INTRODUCTION

The rare earth manganites of the composition R$_{1-x}$A$_x$MnO$_3$ (R=La,Pr,Nd and A=Sr,Ca,Ba) have received great attention worldwide due to its variety of electrical and magnetic properties that depend on the concentration x, temperature, and other parameters.[1] Its colossal magnetoresistance (CMR), for instance, is one of these interesting properties and strongly depends on the dimension of the manganese oxide lattice.[2] In this sense, low dimensional bilayer manganites with the formula R$_{n+1}$Mn$_n$O$_{3n+1}$ (n=2) have attracted considerable interest from the past decade due to their enhanced CMR, significant anisotropic properties, and rich magnetic and resistive phases.[3]

The bilayer manganites are manganese oxides with a layered perovskite structure, where the Mn atom is surrounded by six oxygen ions and forms MnO$_6$ octahedra. The crystal field of oxygen ions splits the degeneracy of the 3d orbital of Mn atoms into threefold degenerate t$_{2g}$ (d$_{xy}$, d$_{yz}$, and d$_{zx}$) and twofold degenerate e$_g$ (d$_{x^2-y^2}$ and d$_{3z^2-r^2}$) orbitals.[4,5] This splitting of degeneracy plays an important role in the properties of manganites. Since the bilayer manganite consists of the ferromagnetic metallic MnO$_2$ bilayers separated by a nonmagnetic (La,Sr)$_2$O$_2$ insulating layer stacked along the c-axis, these are also recognized as an intrinsic ferromagnetic metal (FMM)–insulator (I)–FMM multilayered system. An approach considered to optimize the properties of these materials varies the internal pressure by means of either chemical substitution or external pressure (hydrostatic or uniaxial pressure). Indeed, the transport and

magnetic properties of layered manganites are very sensitive to applied pressure due to the anisotropic compressibility of these materials.[6] There are few studies of the bilayer manganites under hydrostatic pressure,[7,8] and most of them are on La$_{2-2x}$Sr$_{1+2x}$Mn$_2$O$_7$ layered manganites due to its interesting behaviors at low temperatures. We can summarize some important conclusions: (i) the applied pressure leads to a steep drop in resistivity accompanying shifts in transition temperature to high temperature values;[7,8] (ii) Ishihara *et al.*[9] reported that the applied pressure stabilizes the in-plane d$_{x^2-y^2}$ orbital in comparison with the axial d$_{3z^2-r^2}$ orbital for the La$_{2-2x}$Sr$_{1+2x}$Mn$_2$O$_7$ series; (iii) the pressure induced charge transfer from the axial to the in-plane orbital weakens the interbilayer coupling and reduces the charge transport along the c-axis; (iv) the changes in Mn–O–Mn bond angle and Mn–O bond length were observed in the structure of LaSr$_2$Mn$_2$O$_7$ under pressures up to 35 GPa by Kumar *et al.*;[10] and (v) application of pressure leads to a buckling of the Mn–O(3)–Mn linkage in the ab-plane accompanying a compressibility along the c-axis by the interbilayer spacing, as reported by Kamenev[6] concerning the (La$_{0.6}$Nd$_{0.4}$)$_{1.2}$Sr$_{1.8}$Mn$_2$O$_7$ layered manganite.

Another interesting property of bilayer manganite is the tunneling magnetoresistance (TMR) due to its ferromagnetic-insulator-ferromagnetic junction. Kimura *et al.*[11] reported that the applied pressure weakens the interplane magnetic coupling and enhances the interplane TMR for the La$_{2-2x}$Sr$_{1+2x}$Mn$_2$O$_7$ (x=0.3) compound. Since La$_{2-2x}$Sr$_{1+2x}$Mn$_2$O$_7$ is a low dimensional system, it shows a large negative magnetoresistance at a low field.

The crystal structure, electrical transport, and magnetic

---
a)Electronic mail: vanji.hplt@gmail.com.

phases of $La_{2-2x}Sr_{1+2x}Mn_2O_7$ have been investigated using x-ray and neutron diffraction by many research groups.[12–15] Among them, Kubota *et al.*[16] found that the $La_{2-2x}Sr_{1+2x}Mn_2O_7$ system is a FMM in a narrow doping range of $0.30 \leq x \leq 0.48$. Some previous studies reported that $La_{2-2x}Sr_{1+2x}Mn_2O_7$ (x=0.34) undergoes a ferromagnetic to paramagnetic transition at 118 K.[3,16] At temperatures below ~118 K, the magnetic moments on the Mn sites are ferromagnetically coupled both between and within the bilayers. Phase separation scenario, for instance, ferromagnetic metallic and antiferromagnetic charge and orbital ordered insulators, has been studied widely in layered manganites. The results of optical spectroscopic studies by Kunze *et al.*[17] support the phase separation scenario in the x=0.34 compound. They observed two transitions, one near the metal to insulator transition and another at 280 K, reported as anisotropy onset temperature. Charge orders have also been observed above the metal-insulator transition, whereas below this transition the temperature suppresses charge ordering and develops a long-range metallic state.

In this work, hydrostatic pressure and magnetic field effects on electrical transport and magnetization at low temperature in $La_{1.32}Sr_{1.68}Mn_2O_7$ (x=0.34) have been investigated. We have chosen the x=0.34 compound because of its highest T_C and the simplest ferromagnetic coupling between and within the bilayers below T_C. Most of the pressure studies on $La_{2-2x}Sr_{1+2x}Mn_2O_7$ have been done so far for the low doped region ($0.3 \leq x \leq 0.32$), which show a pressure induced antiferromagnetic transition (T_N).[8,18] The increasing pressure induces a segregation into antiferromagnetic electron-rich and ferromagnetic electron-poor Mn_2O_7 layers in the x=0.32 compound.

II. EXPERIMENTAL

The polycrystalline sample of $La_{1.32}Sr_{1.68}Mn_2O_7$ was synthesized by the standard high temperature solid state reaction method. The stoichiometric mixture of La_2O_3, $SrCO_3$, and Mn_2O_3 powders was thoroughly mixed and grounded until the homogenous distribution is achieved. The final mixture was sintered at 1300 °C for 36 h in flowing oxygen. The room temperature powder x-ray diffraction patterns of the final product were recorded with Cu Kα radiation using a Phillips diffractometer in the 2θ range of 20°–80°. The patterns were analyzed with the Rietveld method using the GSAS program.[19] The pressure dependence of resistance was performed up to 25 kbars using a Be–Cu self clamp type hydrostatic pressure cell with Fluorinert 75 as a pressure transmitting medium. Pb and Manganin were used as pressure monometers at low temperature and at room temperature, respectively. The electrical resistivity was measured on a sample of dimension of $1.8 \times 0.9 \times 0.6$ mm^3 by a standard four-probe technique with the electrical contacts made by Pt wire and silver epoxy. A Linear Research (model LR-700) ac-resistance bridge was used to measure the electrical resistance. The temperature was measured by a calibrated Cernox sensor (Lakeshore) and controlled by a Lakeshore (model 340) temperature controller. The temperature stability is better than 1% in the whole temperature range. A normal He^4
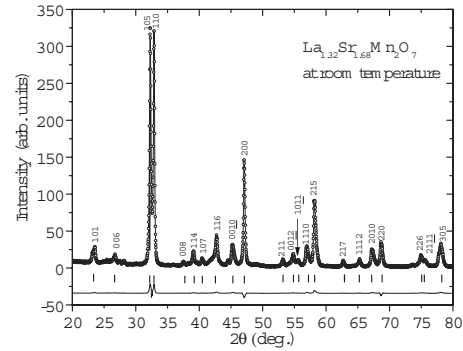

FIG. 1. Powder x-ray diffraction pattern of $La_{1.32}Sr_{1.68}Mn_2O_7$ recorded at ambient pressure and processed by the Rietveld method.

oxford cryostat was used to execute the measurements at low temperature that allows us to reduce the temperature from 300 to 4.2 K and the external magnetic field up to 5 T. We measured both cooling and warming resistances but did not observe any temperature hysteresis. Another miniature hydrostatic pressure cell made of a nonmagnetic Be–Cu alloy suitable to a commercial superconducting quantum interference device magnetometer (Quantum design) was used for magnetization measurements. The measurements were performed at temperatures from 5 to 300 K and at pressures up to 10 kbars. In the measurement, we have also used pure Pb as a pressure monometer.

III. RESULTS AT AMBIENT PRESSURE

Figure 1 shows the x-ray data with refinement for the compound $La_{1.32}Sr_{1.68}Mn_2O_7$. The Rietveld refinement agrees well with the calculated patterns, and the compound was found to be monophasic. The calculated unit cell parameters a=3.8661 Å and c=20.1759 Å are comparable with the values reported by Kubota *et al.*[16] The magnetization in Bohr magnetons per manganese ion as a function of field up to 5 T at low temperature and at room temperature is shown in Fig. 2. The measurements show that the compound is a ferromagnetic at 5 K and a paramagnetic state at room temperature. The ferromagnetic saturation value $3.48\mu_B$ is reasonably consistent with an average Mn valance of +3.4 and a magnetic moment of $3.6\mu_B$ at the Mn site. In Fig. 3, the temperature dependence of the magnetization [field cooled (FC) with 100 Oe] is shown, which results in a sharp ferro-
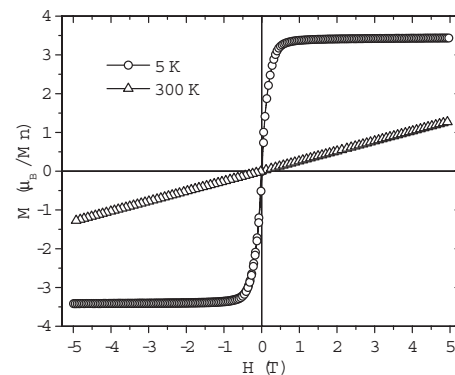

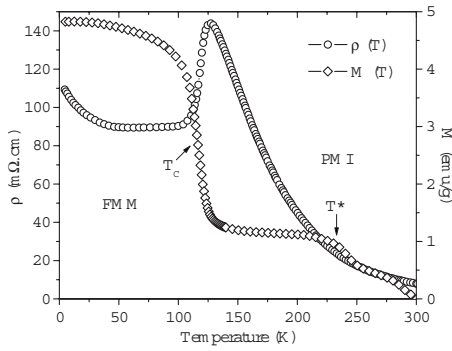FIG. 2. Field dependence of the magnetization curves at 5 and 300 K.

FIG. 3. Temperature dependence of the magnetization under 100 Oe (right scale) and zero field resistivity (left scale).

FIG. 5. Pressure dependence of calculated activation energy (E_a). The inset shows the polaron hopping model fitted in the high temperature regime.

magnetic transition (T_C) at 118 K. Even above the T_C, we have observed another transition at T^*, which was reported earlier.[20,21] There is a two dimensional short-range ferromagnetic order between T_C and T^* temperatures. A sharp metal to insulator transition (T_{MI}) has been observed at 118 K in the temperature dependence of the resistivity curve $\rho(T)$ shown in Fig. 3, which coincides with T_C, a typical example of perovskite manganites. However, we could not observe any transition related to T^* in the $\rho(T)$ curve. The upturn below T_{MI} can be attributed to the two dimensional confinement of the e_g carriers. This resistivity behavior is a typical example of bilayer manganite, and similar upturns of resistivity were observed in other bilayer manganites.[3,22] The low temperature ferromagnetic metallic phase is explained by the double exchange (DE) mechanism,[4] where the hopping of an electron takes place from Mn^{3+} to O^{2-} accompanied by a simultaneous hopping from the latter to Mn^{4+}. The probability of this DE electron transfer of an e_g electron depends on the orientation of the neighboring intra-atomic Hund's coupled t_{2g} spins.[5] High temperature paramagnetic insulating (PMI) phase is explained by the formation of Jahn–Teller polarons due to the distortion of MnO_6 octahedra above T_C.[23] This distortion causes a self trapping of free electrons within the MnO_6 octahedra and forms polarons. The greater distortion results in more trapping of charge carriers.

IV. RESULTS AT HIGH PRESSURE

The increasing pressure significantly affects the transport behavior, as shown in Fig. 4, shifting the transition tempera-

ture (T_{MI}) toward higher temperature values. At a critical pressure $6 \leq P_C \leq 7$ kbars, a second metal-insulator transition (T_{MI}^2) appears at around 90 K. In the inset, we plot the $\rho(T)$ curves for pressures of 3.5, 6.0, and 7.0 kbars in order to visualize the existence of T_{MI}^2. The T_{MI}^1 and T_{MI}^2 are shifted with pressure toward higher temperatures at a rate of 1.7 and 1.3 K/kbar, respectively. The amplitude of the peak of the resistivity curves decreases at rates of -3.63 mΩ/kbar for T_{MI}^1 and -1.04 mΩ/kbar for T_{MI}^2. The insulating behavior is fairly suppressed at around T_{MI}, reflecting the long-range ferromagnetic spin ordering in the respective MnO_2 sheets. When the pressure reaches the maximum available value (25 kbars), the T_{MI}^1 transition is therefore almost suppressed. It is argued that the conductivity in the high temperature paramagnetic region is dominated by polaronic conductions arising from the localized charge carriers due to Jahn–Teller distortion.[24] This polaronic transport in the high temperature region can be characterized by the activation energy (E_a). The Emin–Holstein polaron hopping model with $\rho = AT \exp(E_a/k_BT)$ gives a good fit in the high temperature regime for $\rho(T)$ curves. The calculated E_a values from the fittings are shown in Fig. 5, which indicate that the E_a is reduced from 92 meV for an ambient pressure to 55 meV for 25 kbars. This result implies that the applied pressure reduces the formation of Jahn–Teller polarons.

To confirm whether the pressure induced transition at T_{MI}^2 is magnetic, we have measured the temperature dependence of magnetization under pressure up to 10.2 kbars and have plotted it in Fig. 6. We could not observe any magnetic
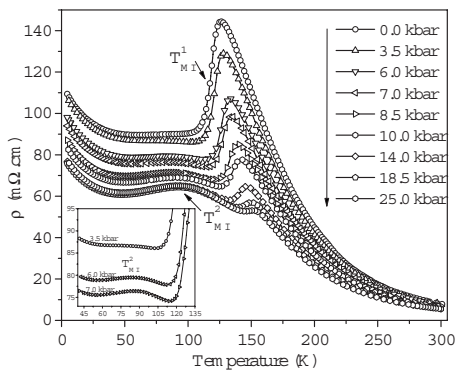

FIG. 4. Temperature dependence of resistivity under different pressures. For better visualization, we show the T_{MI}^2 transition at P_C in the inset.
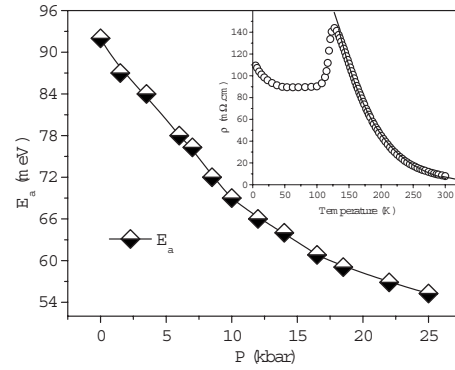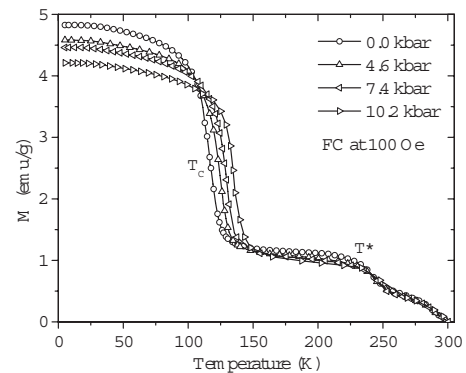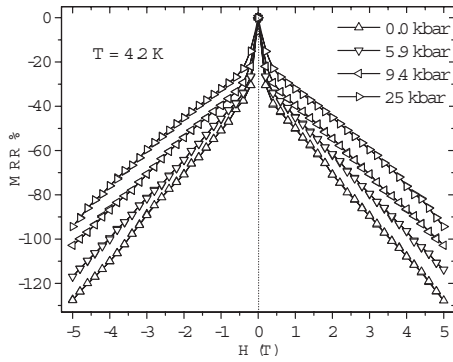

FIG. 6. Temperature dependence of magnetization under different pressures.

FIG. 7. Field dependence of resistivity at different pressures.

FIG. 9. Pressure phase diagram for $La_{1.32}Sr_{1.68}Mn_2O_7$ layered manganite.

transition correspond to T_{MI}^2 in the temperature dependence of magnetization even up to 10.2 kbars. However, increasing pressure shifts the T_C to higher temperature values at the same rate observed for the T_{MI}^1. Both the transition temperatures (T_{MI}^1 and T_C) change equally with pressure at a rate of 1.7 K/kbar. Meanwhile, increasing pressure reduces the magnetic moments significantly at a low temperature ferromagnetic regime.

In Fig. 7, we plotted the field dependence of the resistivity $\rho(H)$ curves, measured at 4.2 K for the pressures 0, 5.9, 9.4, and 25 kbars. In the measurement, we have observed a large negative magnetoresistance on the application of field up to 5 T. The magnetoresistance ratio MRR$=(\rho_0-\rho_H)/\rho_H \times 100$ for the ambient pressure with a 5 T field is about 128%, and it decreases to 95% when the pressure reaches 25 kbars. Also, we have measured the temperature dependence of resistivity $\rho(T)$ under a magnetic field for the same pressures, and the results were plotted in Figs. 8(a)–8(d). We do not observe any transition at 90 K in $\rho(T)$ curves upon the application of a magnetic field up to 5 T at ambient pressure [Fig. 8(a)]. A large negative TMR was observed at T_{MI}^1 in all the pressure range. The MRR of about 300% was observed at T_{MI}^1 for ambient pressure, which is larger than that observed at 4.2 K. The $\rho(T)$ curves for all the pressure range have shown a suppression of T_{MI}^1 at 5 T field, and the increasing pressure reduces the MRR significantly.
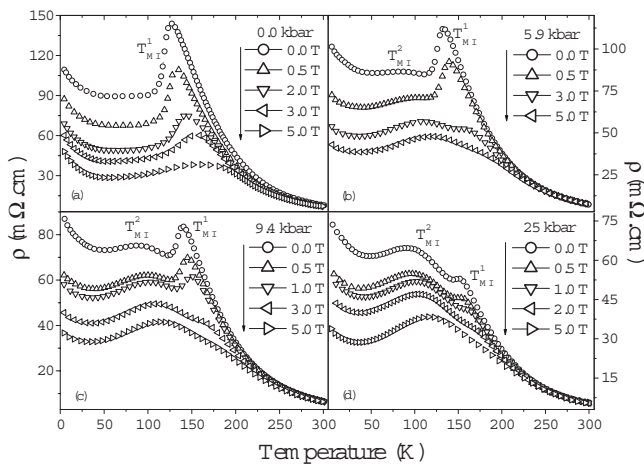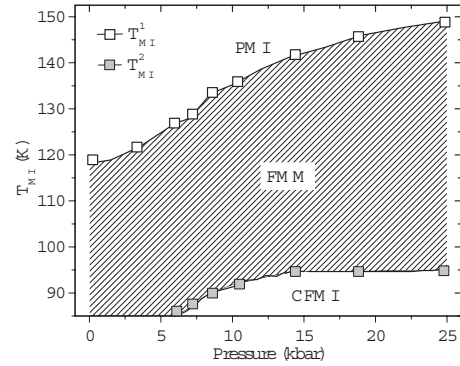

FIG. 8. Temperature dependence of resistivity under pressure and at different values of magnetic field.

V. DISCUSSION

Many groups reported pressure induced antiferromagnetic transition (T_N) in $La_{2-2x}Sr_{1+2x}Mn_2O_7$ (x=0.3 and x =0.32).[8,18] In the present paper (x=0.34), we could not observe any antiferromagnetic transition induced by pressure. The ground state of $La_{2-2x}Sr_{1+2x}Mn_2O_7$ takes consecutively the ferromagnetic state with $d_{3x^2-r^2}/d_{3y^2-r^2}$ orbital ordering for the doping concentration of $0.01 \leq x \leq 0.23$ and the ferromagnetic state with $d_{x^2-y^2}$ orbital ordering for $0.23 \leq x \leq 0.34$.[12] The $La_{1.32}Sr_{1.68}Mn_2O_7$ compound is a simple ferromagnetic coupled bilayer for all the temperature range below T_C. When an external pressure is applied, it is obvious that the Mn–O bond length and the Mn–O–Mn bond angle change significantly,[25,26] which will modify the spin ordering in the MnO_2 layers. According to these changes, the applied pressure can tilt the MnO_6 octahedra that leads to a canted spin state. Canted ferromagnetic arrangements in perovskite manganites have been studied theoretically and experimentally.[27,28] The neutron diffraction measurements reported that a three dimensional spin ordering takes place below T_C, where the magnetic moments cant toward the c-axis with a decrease in temperature. The DE is possible when t_{2g} spins are aligned in a parallel manner. The hopping amplitude $t=t_0 \cos(\theta/2)$ is maximum when the spins are aligned parallel, where θ is the angle between spins placed at the neighboring t_{2g} states.[29] If the spins are aligned antiparallel (t=0), then there is no hopping of electron for DE. In our case, the tilted MnO_6 octahedra does not participate effectively in DE due to its canted spin configuration ($\theta \neq 0$). Thus, we have observed a canted ferromagnetic insulating (CFMI) phase induced by pressure.

Even though the DE model predicts that a canted ferromagnetic state may evolve from an antiferromagnetic state,[27] we are unable to claim the existence of antiferromagnetic state from the pressure dependence of M(T) curves (Fig. 6). Also, the $\rho(T)$ measurement upon application of field [Fig. 8(a)] elucidate our results obtained previously. From the results and considerations described above, we have constructed a pressure phase diagram for $La_{1.32}Sr_{1.68}Mn_2O_7$ layered manganite, as shown in Fig. 9. As seen in the figure, at an ambient pressure there exist two magnetic phases (FMM and PMI). The applied pressure induces a third magnetic phase, known as CFMI, when the pressure reaches a critical value ($6 \leq P_C \leq 7$ kbars). Our results also suggest a possible

pressure induced phase separation scenario with the existence of ferromagnetic metallic and CFMI phases at the low temperature regime. The external pressure suppresses peak resistance monotonically, which is a usual property obtained in magnetic manganites, even though the pressure induced antiferromagnetic superexchange occurred.[7,18] This contradiction may be explained by the pressure enhanced bilayer coupling in the low temperature regime. From our charge transport measurement, we argued that the pressure dependence of T_{MI} changes at P_C without a diminution of the rate of any charge transfer with pressure from ferromagnetic to canted ferromagnetic order.

The external magnetic field increases the alignment of Mn magnetic moments, and the electrical transport across the layer boundaries in these materials is proposed to be due to spin polarized tunneling. We have observed nearly 300% of MRR at T_C with 5 T magnetic field [Fig. 8(a)]. Since the bilayer consists of the FMM–I–FMM junction, the large negative magnetoresistance is explained in terms of the interbilayer TMR effect.[30,31] The TMR mechanism is related to the alignment of the magnetic moments of two consecutinve grains in the ferromagnetic phase at low field, and the other may be due to the changes in the coupling between the ferromagnetic bilayers, which is not clear to occur at low fields but may change with pressure. The ferromagnetically coupled interlayer part acts as a leaky current path along the c-axis. By applying a magnetic field, the magnetization process removes carrier blocking $[(La, Sr)_2O_2]$ boundaries and allows the interbilayer tunneling of spin polarized electrons. However, we observed a decrease in MRR with increasing pressure, this reduction is of 30% compared with ambient pressure. Few studies have been reported on the relative change in spin polarized tunneling with the intralayer orientations.[32,33] The tunneling of electrons is higher when the intralayers are ferromagnetically coupled and lower for the antiparallel orientation. Taking account of the above discussion, such a weakening of MR effect can be explained by the pressure induced CFMI state. Since the pressure induces a canted ferromagnetic spin state in our compound, which is not favorable for the spin polarized tunneling, the tunneling does not take place efficiently at the interlayer. Therefore, the MRR decreases with increasing pressure.

VI. CONCLUSION

In summary, we have synthesized a bilayer manganite and measured the electrical transport and magnetic properties under pressure and magnetic field. The pressure induces a second metal-insulator transition at 90 K. In order to understand the pressure induced metal-insulator transition, we have further measured the temperature dependence of magnetization under pressure. The measurement does not show any transition at 90 K, even up to 10 kbars. It reveals that at high pressure, the low temperature phase is nearly ferromagnetic, but the $\rho(T)$ curve shows that it becomes an insulator. The applied pressure tilted the MnO_6 octahedral, leading to significant changes in the Mn–O–Mn bond angle. These changes established a canted ferromagnetic order, which weakens the DE interaction of electrons. By this way, the

pressure induced a canted ferromagnetic state that leads to an electron localized ferromagnetic insulating behavior. A spin polarized TMR has been observed at T_C upon the external field of 5 T. Pressure reduces the MRR significantly due to the induced canted ferromagnetic spin state. As a result, we conclude the presence of a pressure induced phase segregation between a ferromagnetic metallic and a CFMI phase in the $La_{1.32}Sr_{1.68}Mn_2O_7$ layered manganite.

[1] C. N. R. Rao and B. Raveau, *Colossal Magnetoresistance, Charge Ordering and Related Properties of Manganese Oxides* (World Scientific, Singapore, 1998).
[2] E. Dagotto, T. Hotta, and A. Moreo, Phys. Rep. **344**, 1 (2001).
[3] T. Kimura and Y. Tokura, Annu. Rev. Mater. Sci. **30**, 451 (2000).
[4] C. Zener, Phys. Rev. **82**, 403 (1951).
[5] P. W. Anderson, M. Hill, and H. Hasegawa, Phys. Rev. **100**, 675 (1955).
[6] K. V. Kamenev, M. R. Lees, G. Balakrishnan, D. McK. Paul, W. G. Marshall, V. G. Tissen, and M. V. Nefedova, Phys. Rev. Lett. **84**, 2710 (2000).
[7] Y. Moritomo, K. Hirota, H. Nakao, T. Kiyama, Y. Murakami, S. Okamoto, S. Ishihara, S. Maekawa, M. Kubota, and H. Yoshizawa, Phys. Rev. B **62**, 17 (2000).
[8] K. V. Kamenev, G. J. McIntyre, Z. Arnold, J. Kamarad, M. R. Lees, G. Balakrishnan, E. M. L. Chung, and D. McK. Paul, Phys. Rev. Lett. **87**, 167203 (2001).
[9] S. Ishihara, S. Okamoto, and S. Maekawa, J. Phys. Soc. Jpn. **66**, 2965 (1997).
[10] R. S. Kumar, D. Prabhakaran, A. Boothroyd, M. F. Nicol, and A. Cornelius, J. Phys. Chem. Solids **67**, 2046 (2006).
[11] T. Kimura, A. Asamitsu, Y. Tomioka, and Y. Tokura, Phys. Rev. Lett. **79**, 3720 (1997).
[12] Q. Zhang, W. Zhang, and Z. Jiang, Phys. Rev. B **72**, 142401 (2005).
[13] T. Murata, T. Terai, T. Fukuda, and T. Kakeshita, J. Magn. Magn. Mater. **303**, 138 (2006).
[14] J. F. Mitchell, C. D. Ling, J. E. Millburn, D. N. Argyriou, A. Berger, M. Medarde, D. Miller, and Z. P. Luo, Appl. Phys. A: Mater. Sci. Process. **74**, S1776 (2002).
[15] P. D. Battle, D. E. Cox, M. A. Green, J. E. Millburn, L. E. Spring, P. G. Radaelli, M. J. Rosseinsky, and J. F. Vente, Chem. Mater. **9**, 1042 (1997).
[16] M. Kubota, H. Fujioka, K. Hirota, K. Ohoyama, Y. Moritomo, H. Yoshizawa, and Y. Endoh, J. Phys. Soc. Jpn. **69**, 1606 (2000).
[17] J. Kunze, S. Naler, J. Backstrom, M. Rubhausen, and J. F. Mitchell, Phys. Rev. B **67**, 134417 (2003).
[18] J. S. Zhou, J. B. Goodenough, and J. F. Mitchell, Phys. Rev. B **61**, R9217 (2000).
[19] A. C.Larson and R. B. Von Dreele, General Structure Analysis System (GSAS), Los Alamos National Laboratory Report No. LAUR 86-748, 1994.
[20] A. Wang, G. Cao, Y. Liu, Y. Long, Y. Li, Z. Feng, and J. H. Ross, J. Appl. Phys. **97**, 103906 (2005).
[21] D. N. Argyriou, J. F. Mitchell, C. D. Potter, S. D. Bader, R. Kleb, and J. D. Jorgensen, Phys. Rev. B **55**, R11965 (1997).
[22] Y. Moritomo, Aust. J. Phys. **52**, 255 (1999).
[23] A. J. Millis, P. B. Littlewood, and B. I. Shraiman, Phys. Rev. Lett. **74**, 5144 (1995).
[24] X. J. Chen, C. L. Zhang, C. C. Almasan, J. S. Gardner, and J. L. Sarrao, Phys. Rev. B **67**, 094426 (2003).
[25] D. N. Argyriou, J. F. Mitchell, J. B. Goodenough, O. Chmaissem, S. Short, and J. D. Jorgensen, Phys. Rev. Lett. **78**, 1568 (1997).

[26]D. P. Kozlenko, I. N. Goncharenko, B. N. Savenko, and V. I. Voronin, J. Phys.: Condens. Matter **16**, 6755 (2004).

[27]P.-G. de Gennes, Phys. Rev. **118**, 141 (1960).

[28]D. N. Argyriou, J. F. Mitchell, C. D. Potter, D. G. Hinks, J. D. Jorgensen, and S. D. Bader, Phys. Rev. Lett. **76**, 3826 (1996).

[29]D. S. Dessau and Z. X. Shen, in *Colossal Magnetoresistive Oxides*, edited by Y. Tokura (Gordon and Breach, New York, 1998).

[30]Y. Lu, X. W. Li, G. Q. Gong, G. Xiao, A. Gupta, P. Lecoeur, J. Z. Sun, Y. Y. Wang, and V. P. Dravid, Phys. Rev. B **54**, R8357 (1996).

[31]T. Kimura, Y. Tomioka, H. Kuwahara, A. Asamitsu, M. Murata, and Y. Tokura, Science **274**, 1698 (1996).

[32]M. Julliere, Phys. Lett. **54A**, 225 (1975).

[33]T. Miyazaki and N. Tezuka, J. Magn. Magn. Mater. **139**, L231 (1995).